Examining the Adequacy of the Spectral Intensity Index for Running Safety Assessment of Railway Vehicles during Earthquakes

Xiu LUO[1] and Takefumi MIYAMOTO[2]

[1] *Dr. Eng., Senior Researcher, Structures Technology Division, Railway Technical Research Inst., Tokyo Japan*
[2] *Dr. Eng., Senior Researcher, Railway Dynamics Division, Railway Technical Research Inst., Tokyo Japan*
Email: luo@rtri.or.jp, takefumi@rtri.or.jp

ABSTRACT :

Since the Shinkansen derailment in the 2004 Niigata-ken Chuetsu Earthquake, there has been a strong requirement for railway structures ensuring the running safety of vehicles. This paper examines the seismic behavior of running railway vehicles, and proposes a code-type provision for the Running Safety Assessment (RSA) of vehicles based on the results of comparing the assessment indices of Spectral Intensity (*SI*) and Peak Velocity (*PV*). Moreover, a nomogram based on the *SI* index has been prepared and adopted in a new design code called "Design Standards for Railway Structures and Commentary (Displacement Limits)" [1].

KEYWORDS: vibration displacement, running safety assessment (RSA), spectral intensity (*SI*)

1. INTRODUCTION

In seismic design of railway structures, one of the important tasks is to ensure the running safety of vehicles undergoing seismic motions, which is an essential earthquake-related requirement for railway structures. Running railway vehicles can roll laterally during intense shaking of the ground, thereby inducing large displacement that can cause derailment and/or overturning, which occasionally results in heavy casualties.

Generally, two types of displacement occur at the rail level during earthquakes. One is rail misalignment and/or bending at structural joints, which is caused by track deformation. The other is vibration displacement, even though there may be no obvious deformation of the track. In the case of the former, RSA can be implemented under pseudo-dynamic conditions by comparing the seismic deformation of structures with the limit displacement of vehicles for running safety. For vibration displacement in the latter case, RSA is implemented with the *SI* index (which reflects the relationship between the energy of sinusoidal waves and that of random seismic motions acting on vehicles) according to the Design Standards for Railway Structures and Commentary (Seismic Design) (drawn up by Japan's Railway Technical Research Institute) [2].

However, since the limits of *SI* used in the assessment are based on sinusoidal waves, the irregularity of seismic motion is still not reflected in the RSA. It should also be noted that the *SI* index is not familiar to general designers. To address these problems, this paper examines running safety assessment based on the common *PV* index that is familiar to designers, and compares the assessment results with those obtained by the *SI* index corresponding to various seismic motion types. The results demonstrate that the *SI* index is more appropriate than the *PV* index in terms of accuracy and stability of assessment. Moreover, to enable simple assessment of the running safety for a common seismic design, a nomogram based on the *SI* index without the use of any calculation has been prepared.

2. DIFFERENCE BETWEEN THE *SI* AND *PV* ASSESSMENT INDICES

2.1. SI index based on dynamic response analysis of vehicles using a simplified model

The relative horizontal displacement between the wheel and rail surfaces is an index that enables direct judgment of vehicle derailment. This relative horizontal displacement mainly depends on the absolute response displacement of railway structures. However, structural response displacement obtained in seismic

design is generally relative, meaning that the results cannot be used for RSA. To address this problem, in recent years the authors have proposed an RSA methodology based on the *SI* index which is calculated from the absolute response acceleration of structures [3], [4]. The adoption of the *SI* index is based on the dynamic response analysis of a vehicle based on a simplified model, as outlined below.

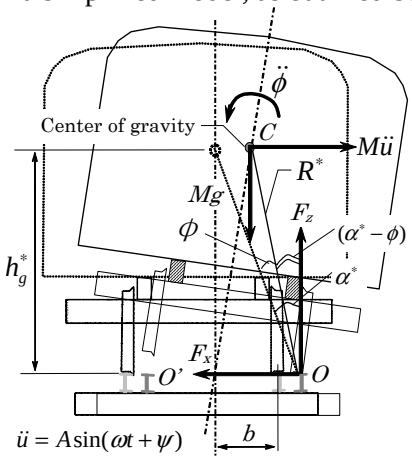

Fig.1 A simplified analytical model for railway vehicles

When the horizontal resistance force between the wheel flange and rail is large enough, the vehicle shown in Fig.1 will oscillate around the centers of rotation *O* or *O'* when it is at the onset of rocking under the horizontal acceleration $\ddot{u}$ acting on the track. The governing equation of the rocking motion is given by

$$I_0\ddot{\phi} + M\ddot{u}R^* \cos(\alpha^* - \phi) + MgR^* \sin(\alpha^* - \phi) = 0 \tag{2.1}$$

where I_0 is the inertia moment of the vehicle about its center of gravity *C*, ϕ is the rocking angle of the vehicle, $\ddot{\phi}$ is the angular acceleration of the vehicle, *M* is the mass of the vehicle, *g* is the acceleration of gravity, $\ddot{u}$ is the horizontal acceleration, R^* is the effective radius for the rotation of the vehicle ($R^* = \sqrt{h_g^{*2} + b^2}$), h_g^* is the effective height of the vehicle's center of gravity taking into account the effects of the overall spring system (the increase in height is about 20%-25% for a vehicle) [5], *b* is half the length of the span between the right/left wheel-rail contact point, and α^* is the angle between R^* and the vertical direction ($\alpha^* \cong b / h_g^*$).

Based on the assumptions that (a) the horizontal acceleration has a half-cycle sine wave form represented by $\ddot{u} = -A\sin(\omega t + \psi)$, and (b) the values of angles α^* and ϕ are small, Equation (1) can then be rewritten in the following form:

$$I_0\ddot{\phi} = -MgR^*(\alpha^* - \phi) + MA\sin(\omega t + \psi)R^* \tag{2.2}$$

Before the onset of rocking, Equation (2.2) can be expressed as $A\sin(\omega t + \psi) = g\alpha^*$, and when $t = 0$ the equation becomes $A = g\alpha^* / \sin\psi$. When the variables are substituted into Equation (2.2), the following expression is derived:

$$\ddot{\phi} - p^2\phi = \alpha^* p^2 \left[\frac{\sin(\omega t + \psi)}{\sin\psi} - 1\right] \tag{2.3}$$

After the variable $p^2 = MgR^* / I_0$ and the initial condition ($\phi_{(t=0)} = 0$, $\dot{\phi}_{(t=0)} = 0$) are substituted into Equation (2.3), the solution for the differential equation is obtained. In fact, the condition necessary for the onset of vehicle overturn is that the vehicle's center of gravity rotates to a position just over the center of rotation *O* ($\phi = \alpha^*$). After this condition is substituted into the solution of Equation (2.3), the solution can be simplified as the very brief form shown in Equation (2.4) [6],[7],

$$\frac{A}{g\alpha^*} = \sqrt{1 + \left(\frac{\omega}{p}\right)^2} \tag{2.4}$$

where $A/(g\alpha^*)$ is the normalized amplitude of input acceleration and ω/p is the normalized frequency of input waves.
Furthermore, Equation (2.4) can be approximately expressed in the following form, because $(\omega/p)^2 >> 1$ in general cases.

$$\frac{A}{\omega} = \frac{g\alpha^*}{p} \tag{2.5}$$

Equation (2.5) expresses the minimum velocity (i.e. the critical velocity) needed to induce the initial overturning of the vehicle. This movement energy created by the critical velocity is equal to the critical potential energy needed for the initial overturning. The critical potential energy is represented by the rocking of the center of gravity *C* of the vehicle to the highest position, i.e. right above point *O* in Fig.1. The relationship between the critical energy of the movement and the potential energy can be expressed by the response spectrum of velocity. Since this represents the maximum response values of velocity, it is in theory closely related to the maximum potential energy of the input wave as described below.

In general, the variables used in the response spectrum of a vibration system are assumed as the mass of the system $\overline{M}$, the spring factor $\overline{K}$, the natural frequency $\overline{\omega}$, the maximum displacement $x_{\max}$, the displacement response spectrum S_d and the velocity response spectrum S_v. Consequently, the maximum potential energy can be expressed as $1/2(\overline{K}x^2_{\max})$. As $x_{\max} = S_d$ and $S_v \cong \overline{\omega} S_d$, the maximum potential energy per unit mass is given by

$$\frac{1}{2}(\overline{K}/\overline{M})S_d^2 = \frac{1}{2}S_v^2 \tag{2.6}$$

From Equation (2.6), it is clearly understood that the velocity response spectrum is directly related to the spectrum of the maximum potential energy. The index for the RSA is therefore liable to be determined by the velocity response spectrum, which is the origin of the *SI* index.

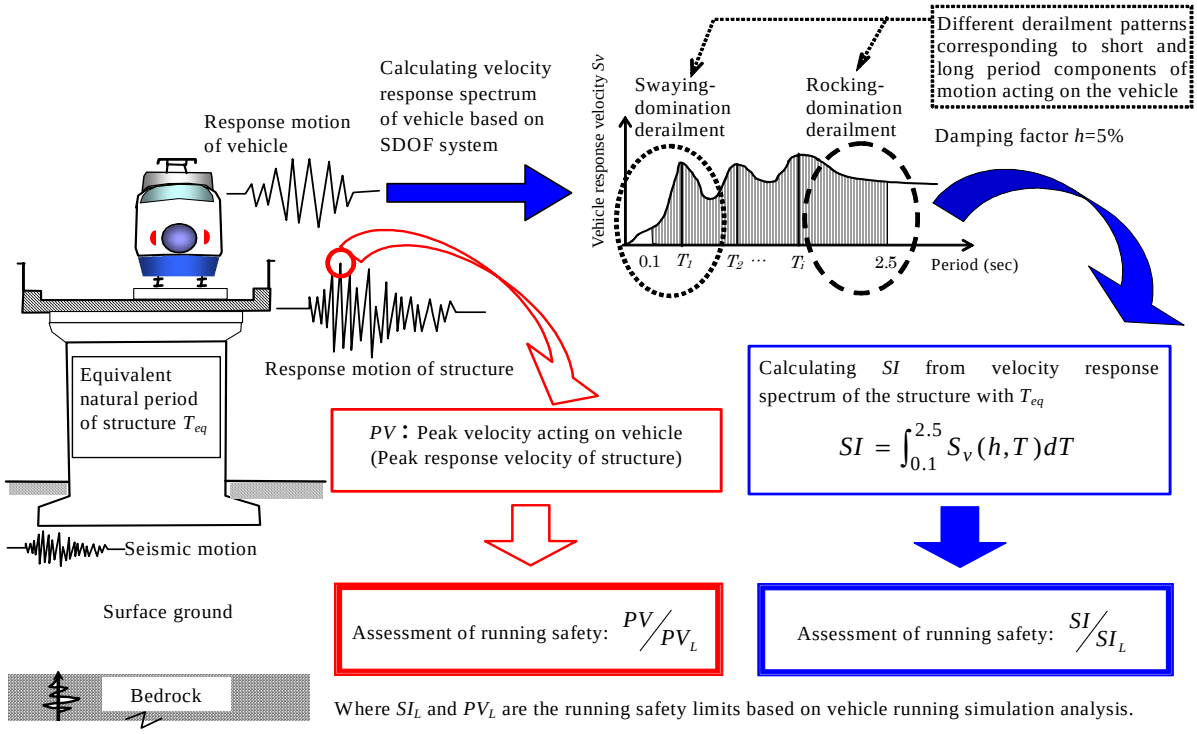

Fig. 2 Procedure for RSA of vehicles using *SI* and *PV* indices

2.2. Running safety assessment using SI and PV indices

The *SI* is an energetic index that reflects the intensity of vehicle response. As shown in Fig. 2, the *SI* is calculated by integrating the velocity response spectrum from the period of 0.1 sec to 2.5 sec, which represents the energy summation of the response. The range of integration is decided on the basis of the response

characteristics of vehicles and structures. In the figure, the difference between the *SI* and *PV* indices is also shown. In contrast with the frequency-domain *SI* index, which reflects the output intensity from the vehicle, *PV* is a time-domain index reflecting the intensity (peak velocity) acting on the vehicle.

Another reason to choose *SI* is the different patterns of derailment corresponding to different period components of the motion acting on the vehicle, as shown in Fig. 2. In the zone with short-period components, the wheel flange comes into collision with the rail, and large lateral forces are generated at the contact points. In this case, swaying-domination derailment may occur (also known as higher-center rolling) around the center of gravity *C* in Fig.1. In the zone with long-period components, however, rocking-domination derailment may occur (also known as lower-center rolling) around centers *O* or *O'* in Fig.1. During an earthquake, the response of the vehicle is a mixture of the components corresponding to short and long periods. It is therefore rational to evaluate the total energy by integrating the velocity response spectrum from the short period to the long period as shown in Fig. 2.

3. COMPARISON OF *SI* AND *PV* FOR RSA

3.1. Seismic motion selection and structural response calculation

This paper examines the adequacy of the *SI* and *PV* indices from the viewpoint of accuracy and stability for the assessment of running safety. Firstly, a number of typical seismic motions were selected and structural responses were calculated. Secondly, vehicle derailment limits were judged on the basis of vehicle running simulation using structural response waves. Finally, the limit values of *SI* and *PV* were compared, focusing on accuracy and stability for the RSA.

The characteristics of 11 seismic motions used in the examination are shown in Table 3.1. These typical seismic motions were picked up from an earthquake database by considering the source property, epicenter distance, transmission behavior, classification of surface ground etc. A Single-Degree-Of-Freedom (SDOF) system with damping factor h=5% was applied to the structural response calculation. Since the maximum amplitudes of the seismic motions shown in Table 3.1 are not the same, the values were normalized to 100 gal by adjustment coefficient multiplication. The absolute acceleration response motions at the crest of the structure were then calculated by inputting the normalized seismic motions. Finally, the acceleration motions were filtered using a high-pass 0.1-Hz filter, and were integrated with the displacement motions assumed to be the acting motions for vehicle running simulation.

Table 3.1 Characteristics of seismic motions used in adequacy examination of *SI* and *PV*

Earthquakes	Seismic motion	Characteristics
Kushiro-oki	Kushiro-kisyoudai-NS Kushiro-kisyoudai-EW	Deep epicenter, long duration, dominated by short periods
Hokkaido-Tohooki	Urawa-EW Urawa-NS	Large earthquake, far away
Hyogoken-nanbu	Kobe-kaiyokisyoudai-NS Kobe-kaiyokisyoudai-EW	Near-source large earthquake, short duration, dominant around periods of 1.0 sec, large influence on structures and vehicles due to large velocity
Taiwan-chichi	Taichuuken-TCU068	Near-source earthquake, dominant around periods of 3.0-5.0 sec, pulse-shaped large-velocity wave
L1-design	L1-G3	Design seismic motion of common surface ground for L1 earthquake
L1-design	L1-G5	Design seismic motion of soft surface ground for L1 earthquake
L2-design	L2-Spec Ⅰ-G3	Design seismic motion of common surface ground for L2 interplate earthquake
L2-design	L2-Spec Ⅱ-G3	Design seismic motion of common surface ground for L2 near-source earthquake

3.2. Vehicle running safety limits based on rigorous numerical simulation

Fig.3 shows a proposed rigorous numerical model for vehicle running simulation that is capable of dealing with large displacement of vehicle [8]. It is represented by seven mass elements (a body, two tracks and four wheel-sets) with 42 degrees of freedom, and eight wheels supported by rails with 16 degrees of freedom in the horizontal and vertical directions. The vehicle model consists of 58 degrees of freedom in total. In the simulation, the lateral displacement between the wheel tread center and rail was adopted to evaluate the critical condition of running safety against shaking on the track. The limit value of this lateral displacement was set at ±70 mm as shown in Fig.4.

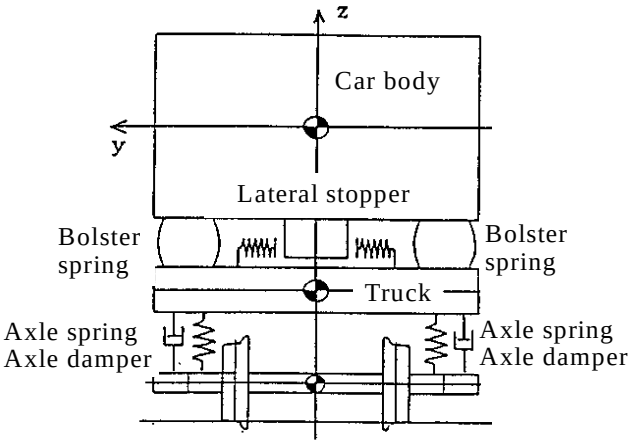

Sectional view of vehicle at the back of running direction

Fig.3 Standard for derailment judgment

Given in Fig.5 are the running safety limits calculated on the basis of the vehicle running simulation with the 11 seismic motions shown in Table 3.1. As shown in Fig.5 (a), there is a big difference in the safety limit magnification corresponding to the various seismic motions because of their different period characteristics. Fig.5 (b) gives the safety limit amplitudes of the seismic motions, calculated on the basis of the magnifications shown in Fig.5 (a). The figure indicates the maximum displacement amplitudes for running safety corresponding to the equivalent natural periods of structures.

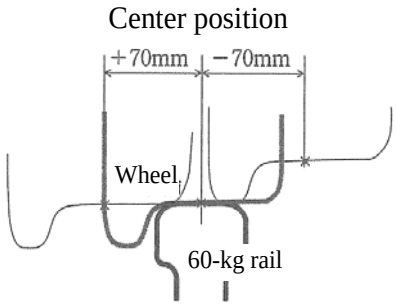

Fig.4 Standard for derailment judgment

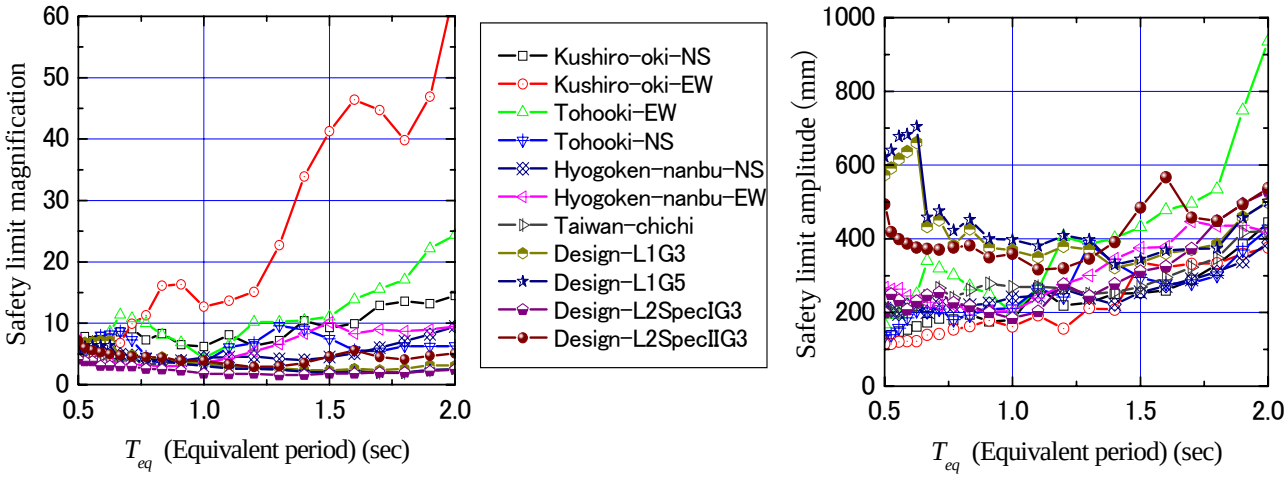

(a) Safety limit magnification (b) Safety limit amplitude

Fig.5 Safety limits from running simulation (rail/wheel horizontal displacement: ±70 mm)

3.3. Examining the stability of SI and PV safety limits

Because the stability of safety limits is important in RSA, the variation coefficients of the *SI* and *PV* safety limits were examined. To consider the correspondence with a series of current investigations, in this examination the limit value of displacement between the wheel and the rail was set at 25 mm in the vertical

direction for derailing judgment. Given in Fig.6 is the method for calculating the safety limit of *SI* (SI_L). The calculation procedure is described below.

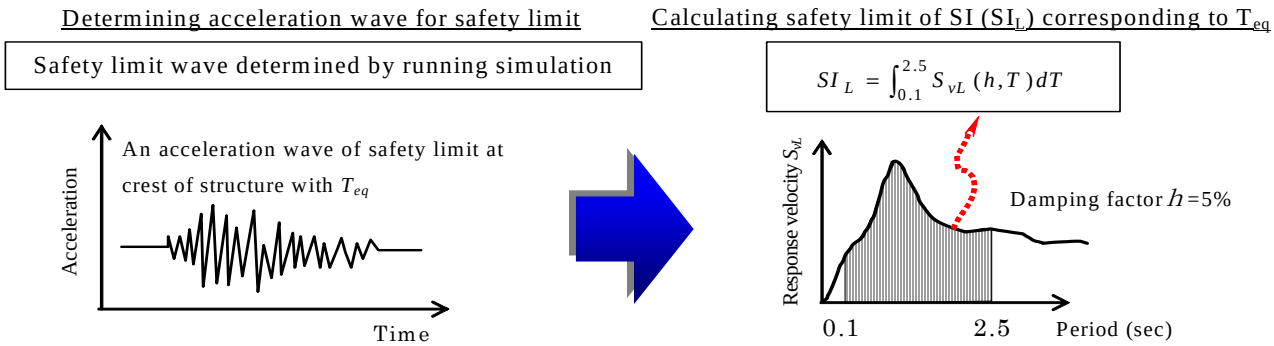

Fig.6 Method for calculating safety limit of *SI* (SI_L)

i) An acceleration wave of the safety limit at the crest of a structure with T_{eq} was determined on the basis of the magnification shown in Fig.5 (a), obtained by vehicle running simulation.
ii) From this wave, the limit velocity response spectrum was calculated by adopting a damping factor of h=5%.
iii) The safety limit SI_L was calculated by integrating the response velocity S_{vL} from 0.1 sec to 2.5 sec as shown in Fig.6.

After steps i) to iii) were repeated, the safety limits SI_L for RSA were made out for all the equivalent natural periods involved in the seismic design of structures.
With regard to calculation of the safety limit of *PV* (PV_L), the values were obtained by multiplying the safety limit magnifications shown in Fig.5 (a) with the structure velocity response waves calculated by inputting the normalized seismic motions.

Given in Fig.7 are safety limits SI_L and PV_L calculated on the basis of vehicle running simulation. To compare the stability of the two safety limits, the corresponding coefficients of variation are plotted together in the figures. It is clearly understood that the average coefficient of variation for SI_L is about 0.1 (Fig.7 (a)), which is much smaller than the value of about 0.3 to 0.5 for PV_L (Fig.7 (b)). In terms of accuracy and stability for RSA, therefore, safety limit SI_L is more adequate than PV_L.

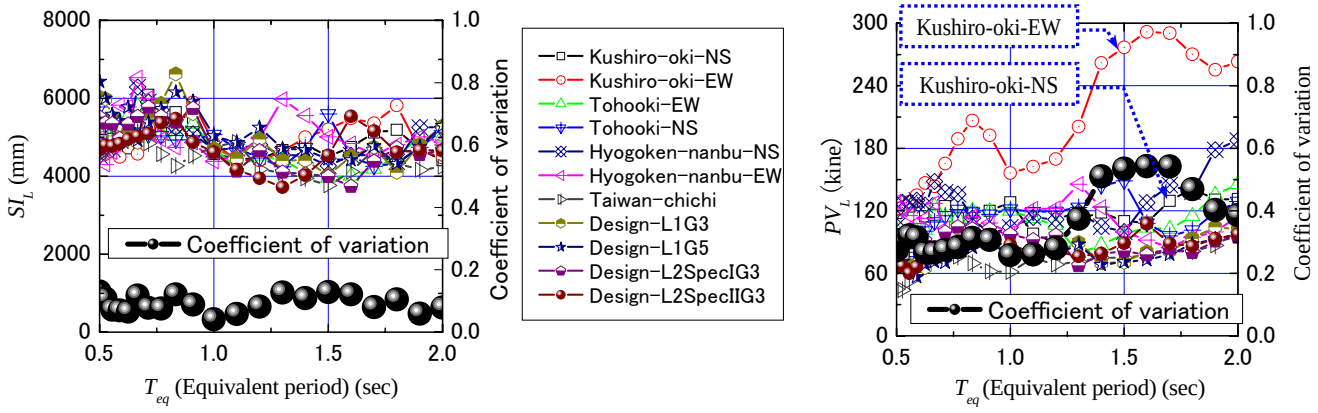

(a) Safety limit SI_L (b) Safety limit PV_L

Fig.7 Safety limits SI_L, PV_L and coefficients of variation (rail/wheel vertical displacement: 25 mm)

3.4. Examining the influence of seismic motion characteristics

With regard to the safety limit PV_L shown in Fig.7 (b), the limit values corresponding to seismic motion Kushiro-oki-EW are extremely high. To investigate the cause, a comparison with seismic motion Kushiro-oki-NS resulting from the same earthquake was implemented in terms of the characteristics of time

history and period component. The wave shape of the two normalized seismic motions (with a peak acceleration of 100 gal) and their Fourier spectra are given in Fig.8. From the figure, it can be seen that the short-period components of the EW wave are more dominant than those of the NS wave. Particularly, the close-up of the EW wave clearly shows that the short-period components are superimposed on the long-period components at times of about 20.7 sec and 21.8 sec, which indicates the dominant characteristics of the short-period components. Moreover, the Fourier spectra shown in Fig.8 (b) also reveal that the short-period components of the EW wave are stronger than those of the NS wave, but the long-period components of the EW wave are much weaker than those of the NS wave.

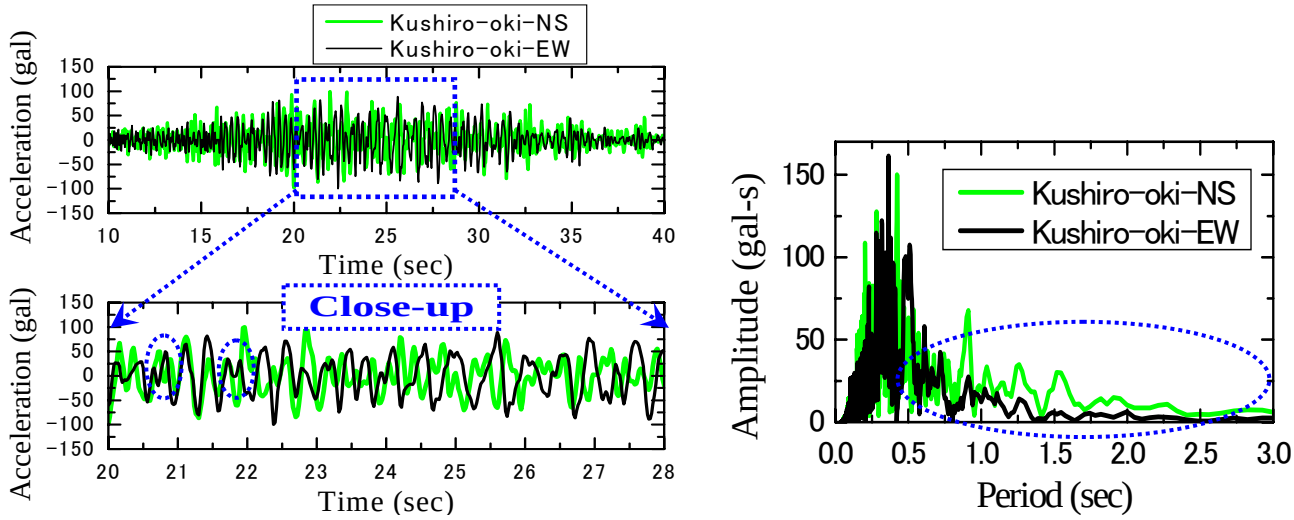

(a) Wave shape of time history (b) Fourier spectra

Fig.8 Comparison of Kushiro-oki-NS and EW in terms of wave shape and period component

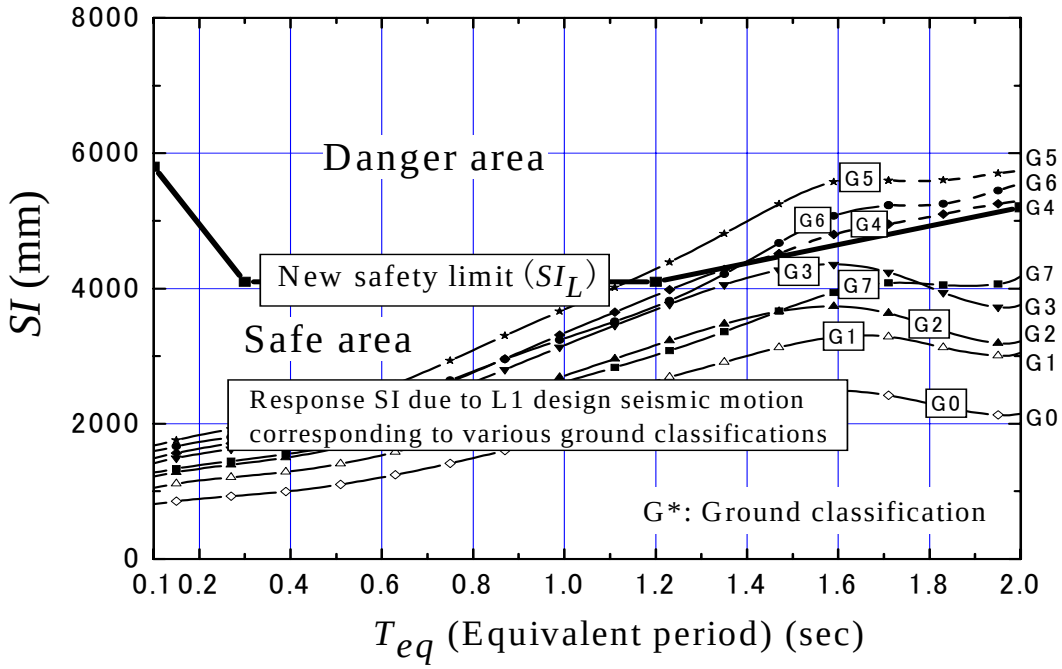

Fig.9 Nomogram for RSA corresponding to various ground classifications

4. APPLICATION TO SEISMIC DESIGN OF STRUCTURES

Although the proposed method for RSA based on the stable *SI* index has been shown to be appropriate for the seismic design of structures, from the viewpoint of engineering practice it is still inconvenient that the values of

response *SI* and the limit SI_L should be calculated through dynamic analysis of structures and vehicle running simulation. It is therefore necessary to provide a convenient code-type method for seismic design. For quick assessment of running safety, a nomogram (for which no calculation is needed) has been made as shown in Fig.9. In this nomogram, the line labeled *new safety limit* (SI_L) is an envelop of a number of safety limits calculated using the 11 seismic motions shown in Table 3.1. In contrast to the old limit line shown in the Design Standards for Railway Structures and Commentary (Seismic Design) [2] (which is based on sinusoidal waves), the new limit line (reflecting earthquake irregularities due to source property, epicenter distance, transmission behavior etc.) is based on the representative seismic motions. Moreover, the curves of response *SI* plotted in the nomogram are calculated using the L1 design seismic motions corresponding to various ground classifications [2]. In seismic design, if the equivalent natural period T_{eq} of the objective structure and the ground classification are known, the running state of the vehicle can be evaluated by comparing the quantities of response *SI* with SI_L.

5. CONCLUSIONS

The important task of assessing vehicle running safety in an earthquake is significant to the seismic design of railway structures. To develop a code-type provision for RSA, this study examines the behavior of running vehicles subjected to seismic motion, and compares the characteristics of the *SI* and *PV* assessment indices corresponding to a range of seismic motions. The results demonstrate that the *SI* index is more appropriate than the *PV* index from the viewpoint of accuracy and stability of assessment. Moreover, to enable simple assessment of running safety for a common seismic design, a nomogram with the limit SI_L and the response *SI* plotted together has been made.

Finally, the RSA method established in this study has been adopted in a new design code called “Design Standards for Railway Structures and Commentary (Displacement Limits)” [1], which was published recently.

REFERENCES

[1] Railway Technical Research Institute (2006). Design Standards for Railway Structures and Commentary (Displacement Limits). Maruzen Co., Ltd., Tokyo, (in Japanese).
[2] Railway Technical Research Institute (1999). Design Standards for Railway Structures and Commentary (Seismic Design). Maruzen Co., Ltd., Tokyo, (in Japanese).
[3] Luo, X. (2005). Study on Methodology for Running Safety Assessment of Trains in Seismic Design of Railway Structures,” *Journal of Soil Dynamics and Earthquake Engineering*, **25:2**, Elsevier Science Ltd., pp.79-91.
[4] Luo, X. (2003). A practical Methodology for Running Safety Assessment of Trains during Earthquakes Based on Spectral Intensity. *Proc. of the IABSE Symposium Antwerp 2003*, CD-ROM (Outline pp.322-323), Belgium.
[5] Kunieda, M. (1972). Theoretical Study on the Mechanics of Overturning of Railway Rolling Stock. *Railway Technical Research Report*, RTRI, **793**: 1-15, (in Japanese).
[6] Ishiyama, Y. (1982). Criteria for Overturning of Bodies by Earthquake Excitation. *Transactions of the Architectural Institute of Japan*, **317**: 1-12.
[7] Luo, X. (2002). A Code-type Provision for Running Safety Assessment of Trains Subjected to Earthquake Motion. *Proc., 12th European Conference on Earthquake Engineering*. Paper Reference 462 (CD), London, U.K.
[8] Miyamoto, T., Ishida H., and Matsuo, M., (1997). Running Safety of Railway Vehicle as Earthquakes Occur. *Quarterly Report of RTRI*, **38:3**, 117-22.